Ligand-Doped Liquid Crystal Sensor System for Detecting Mercuric Ion in Aqueous Solutions

ARTICLE *in* ANALYTICAL CHEMISTRY · MARCH 2015

Impact Factor: 5.64 · DOI: 10.1021/acs.analchem.5b00675 · Source: PubMed

4 AUTHORS, INCLUDING:

Chih-Hsin Chen
Tamkang University
26 PUBLICATIONS **588** CITATIONS
SEE PROFILE

Adam Lee
Tamkang University
66 PUBLICATIONS **621** CITATIONS
SEE PROFILE

analytical chemistry

Article

pubs.acs.org/ac

Ligand-Doped Liquid Crystal Sensor System for Detecting Mercuric Ion in Aqueous Solutions

Chih-Hsin Chen,* Yi-Cheng Lin, Hao-Hsiang Chang, and Adam Shih-Yuan Lee*

Department of Chemistry, Tamkang University, New Taipei City 25137, Taiwan

Supporting Information

ABSTRACT: We developed a liquid crystal (LC) sensor system for detecting mercuric ion (Hg^{2+}) in aqueous solutions. In this system, 4-cyano-4′-pentyl biphenyl (5CB) was doped with a sulfur- and nitrogen-containing ligand 5-(pyridine-4-yl)-2-(5-(pyridin-4-yl)thiophen-2-yl)thiazole (ZT) as the Hg^{2+} specific LCs. When the system was immersed in the solution containing Hg^{2+}, the complex of ZT and Hg^{2+} formed, which disrupted the orientation of LC and lead to a dark-to-bright transition of the image of LCs. From mercuric binding titrations monitored by UV−vis spectroscopy, it was found that 1:1 Hg^{2+}/ZT complexes were formed. The limit of detection (LOD) of the system to Hg^{2+} is 10 μM, and it did not respond to Cd^{2+}, Zn^{2+}, Cu^{2+}, Pb^{2+}, Fe^{+}, Mg^{2+}, Ca^{2+}, Na^{+}, and K^{+}. Besides, we also demonstrated that this system is capable of detecting Hg^{2+} in tap water and pond water. Because the signal of this system is colorful under ambient light, which is readily understood by normal users, it can be used as a portable device to monitor the water quality at any location.

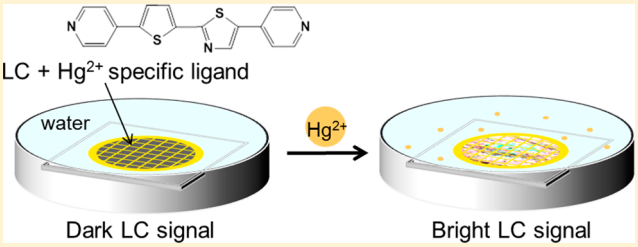

Mercury contamination in water has been considered as a serious problem to human health due to its high toxicity. The accumulation of mercury in the human bodies over time may cause serious mental and central nervous illness.[1] Therefore, preventing water from mercury contamination is a very important task to human society and it requires an efficient analytical method to detect mercury in water. Currently, the most accurate and reliable technique to detect mercuric ion (Hg^{2+}) in water are atomic absorption spectrometry,[2,3] cold vapor atomic fluorescence spectrometry,[4,5] gas chromatography,[6,7] liquid chromatography,[8,9] and capillary electrophoresis.[10,11] However, all of them need sophisticated instruments, which make them not suitable for fast, real-time, and continuous monitoring of water quality in the field. Therefore, the chemical sensor system has been considered as a more applicable method to overcome such limitations because it usually applies portable techniques such as electrochemistry,[12,13] colorimetry,[14,15] or fluorometry[16,17] to produce the signals. Nevertheless, they still need an electrical device as the signal read-out system such that they are not ideal for untrained personnel.

Beyond those well-developed electrochemical or optical techniques, LC-based sensor is considered as a new type of label-free and portable technique for detection because it can be operated under ambient light without using bulky and expensive instrumentation.[18−22] Although the LC-based sensor has been applied for the detection of different analytes such as oligonucleotides,[23,24] proteins,[25,26] proteases,[27,28] viruses,[29,30] organophosphates,[31] and amines,[32,33] the study using this system to detect heavy metals is still rare. For example, Hu et al. reported the LC-based sensor for the detection of Cu^{2+} using surface-immobilized urease.[34] This sensor applied an LC/aqueous system by using a urease-modified gold grid confined with a thin layer of nematic LC, 4-cyano-4′-pentyl biphenyl (5CB) mixed with 4-cyano-4′-biphenylcarboxylic acid (CBA) where the orientation of LC is sensitive to pH. When the sensor was immersed in a urea solution, urea was hydrolyzed by urease to produce ammonia. The ammonia was then ionized into ammonium and hydroxide ions which increased the pH of solution, resulting in a reorientation of LC from planar to homeotropic. Therefore, a bright-to-dark transition of LC image was observed under polarized light. The presence of Cu^{2+} effectively inhibited the activity of urease, which caused another reorientation of LC from homeotropic to planar so a dark-to-bright transition of LC image was observed. The detection is real time in this system, and it can detect Cu^{2+} in the concentration level of ppm. However, this system was not applicable for heavy metals with higher toxicity such as cadmium, mercury, lead, and arsenic. More recently, Yang et al. reported an LC-based biosensor to detect Hg^{2+} by using oligonucleotide as recognition units through the specific binding of Hg^{2+} to two DNA thymine (T) bases.[35] In their system, the presence of Hg^{2+} in aqueous solution leads to a conformational reorganization of the oligonucleotide probes from the hairpin structure to duplex-like complexes. When the duplex-like complexes are then bound on the substrate modified with capture probes, the orientation of LC is disrupted and a bright LC image was observed as a result. The limit of detection (LOD) of this system to Hg^{2+} can be as

Received: February 17, 2015
Accepted: March 31, 2015
Published: March 31, 2015

DOI: 10.1021/acs.analchem.5b00675
Anal. Chem. 2015, 87, 4546−4551

low as 0.1 nM (equals to 0.02 ppb), showing that heavy metals can also be detected by the LC sensor system with high sensitivity through the formation of complex which amplifies the signals. However, this sensor applied LC/solid system requires additional procedures to fabricate an LC cell. Therefore, the detection of this system is not real time.

Among previous studies on the mercury sensor system, small-molecule ligands are mostly applied as the probe to capture Hg^{2+} in aqueous solution.[36,37] The small molecule ligand can be a chromophore itself or be covalently linked to a chromophore. The specific binding of Hg^{2+} to the ligand induces the perturbation of a chromophore and leads to the change of UV−vis or fluorescence signal in the solution. The advantages of using small-molecule ligands as the probe of sensor include high selectivity and affinity which can be achieved through proper design of the molecular structure of the ligand. For example, Nolan et al. reported a turn-on fluorescent sensor for detecting Hg^{2+} by using a small-molecule ligand based on a 3,9-dithia-6-azaundecane moiety covalently linked to an aniline-derived seminapthofluorescein chromophore.[17] Besides, Han et al. utilized the idea that Hg^{2+} and DNA thymine bases (T) form a stable T−Hg^{2+}−T complex to design a small-molecule ligand for Hg^{2+} sensing by linking two thymine moieties to the perylene backbone.[38] However, the photophysical properties of these ligands are pH sensitive, which increases the difficulty to detect Hg^{2+} precisely in aqueous solutions with different pH values. In addition, the small-molecule ligand must be water-soluble for detecting of Hg^{2+} in aqueous solution. To the best of our knowledge, the small-molecule ligand has never been applied in the LC sensor system for detecting Hg^{2+} so far.

In this study, we synthesized a small-molecule ligand 5-(pyridin-4-yl)-2-(5-(pyridin-4-yl)thiophen-2-yl)thiazole (ZT) which is composed of two pyridine, one thiazol, and one thiophene moieties. The binding affinity between Hg^{2+} and nitrogen or sulfur atoms has been widely reported previously.[39−42] We anticipate that ZT is capable to selectively bind to Hg^{2+} in aqueous solution and form complexes which can further lead to the change of optical signals in the LC system. The binding stoichiometry and mode of ZT to Hg^{2+} were studied by UV−vis spectrometry and NMR, respectively. Furthermore, ZT was doped into 5CB to develop an LC-based sensor system and the specificity and sensitivity of this system for detecting Hg^{2+} in aqueous solutions were investigated. Because the LC system applied an LC/aqueous interface for the metal−ligand binding, the water solubility and the pH sensitivity of the ligands will not be the problem for detection.

EXPERIMENTAL SECTION

Materials and Instruments. Glass slides were obtained from Fisher Scientific. Mercury perchlorate hydrate and all other metal chlorides were purchased from Sigma-Aldrich. Liquid crystal 4-cyano-4′-pentylbiphenyl (5CB) was purchased from TCI (Taiwan). 5-Bromo-2-(5-bromothiophen-2-yl)-thiazole[43] and 4-(tributyltannyl)pyridine chloride[44] were synthesized based on the procedures described in a previous paper. Water was purified by using a Milli-Q system (Millipore). Tap water and pond water were collected in the campus of Tamkang University. The UV spectra were measured by using a Thermo Scientific Evolution 60S UV−vis spectrophotometer. The NMR spectra were recorded on a Bruker AC-300 FT-NMR spectrometer.

Synthesis of ZT. The mixture of 5-bromo-2-(5-bromothiophen-2-yl)thiazole (1.0 equiv) and 4-(tributylstannyl)pyridine chloride (3.0 equiv), triethylamine (6.0 equiv), and tetrakis-(triphenylphosphine) palladium (6.0%) were allowed to react in dry DMF at 120 °C for 48 h. After cooling, the solution was filtered and quenched by water. After that, the solution was extracted three times with dichloromethane. The combined organic extracted was washed with brine and dried over $MgSO_4$. The solvent was removed under reduced pressure, and the crude product was further purified by column chromatography by using dichloromethane/hexane (1:1) as the eluent followed by recrystallization by dichloromethane and hexane to yield ZT as an orange-yellow solid. ^{1}H NMR (300 MHz, $CDCl_3$): δ 8.64−8.67 (m, 4H), 8.14 (s, 1H), 7.58 (d, 1H, J = 3.6 Hz), 7.50−7.52 (m, 3H), 7.46 (dd, 2H, J = 1.6, 6.2 Hz). ^{13}C NMR (75.5 MHz, CD_2Cl_2): δ 161.6, 155.4, 150.5, 143.5, 141.2, 140.2, 138.1, 136.3, 132.7, 128.1, 126.2, 120.4, 119.6. FABMS (m/z): 321 [M^+]; HRMS (m/z): calcd for $C_{17}H_{11}N_3S_2$, 321.0394; found, 321.0377.

Binding Study of ZT and Hg^{2+} by Using UV−Visible Spectrometry. The UV−vis spectra of ZT (50 μM in methanol) containing different concentrations of Hg^{2+} (25−200 μM) were measured. A Job plot of the ZT−Hg^{2+} complex was obtained by plotting the absorption intensity against the molar fraction of ZT when the total concentration of solution was fixed at 40 μM. The binding constant of the ZT−Hg^{2+} complex was determined based on the Benesi−Hildebrand equation[45] where I is the absorption intensity at 402 nm at any concentration of Hg^{2+} and I_0 is the absorption intensity at 402 nm in the absence of Hg^{2+}.

Preparation of DMOAP-Coated Slides. To clean the surface, glass slides were immersed in a 5% Decon-90 solution (a commercially available detergent) for 2 h, sonicated in DI water for 15 min, and rinsed thoroughly with DI water twice. After this, the slides were dried under a stream of nitrogen. The cleaned glass slides were immersed in an aqueous solution containing 0.1% (v/v) DMOAP for 8 min and then rinsed with copious amounts of DI water. DMOAP-coated slides were dried under a stream of nitrogen and heated in a 100 °C vacuum oven for 15 min.

Preparation of LC Sensor System. TEM copper grids (75 mesh, Electron Microscopy Sciences) were cleaned in methanol, ethanol, and acetone (sonicated in each solvent for 15 min) and then heated overnight at 100 °C to evaporate residual solvent. To prepare LC sensor system, a copper grid was placed on the a piece of DMOAP-coated slide (5 mm × 5 mm), and approximately 0.3 μL of 5CB doped with 0.3 wt % of 5-(pyridine-4-yl)-2-(5-(pyridin-4-yl)thiophen-2-yl)thiazole (ZT) was dispensed onto the grid. Excessive LC was removed by using a capillary tube. Finally, the grid containing ZT-doped LCs was immersed in 300 μL of aqueous solution containing various metal ions. The optical appearances of these samples were observed by using a polarizing optical microscope (Canon EOS D650, Japan) in the transmission mode. Each image was captured with a digital camera mounted on the microscope with an exposure time of 1/80 s.

RESULTS AND DISCUSSION

Synthesis of ZT. Scheme 1 illustrates the key reaction for the synthesis of ZT applied in this study. The ammonium salt of 4-(tributylstannyl)pyridine was allowed to react with 5-bromo-2-(5-bromothiophen-2-yl)thiazole via a palladium-catalyzed Stille coupling reaction. Here, 2 equiv of trimethylamine

DOI: 10.1021/acs.analchem.5b00675
Anal. Chem. 2015, 87, 4546−4551

Scheme 1. Synthetic Route of ZT

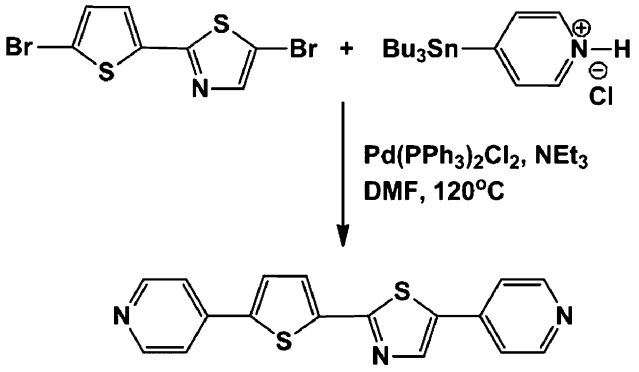

was added for the deprotonation of ammonium salt of 4-(tributylstannyl)pyridine to yield ZT in good yield (~60%). The compound was soluble in common organic solvents such as chloroform, dichloromethane, tetrahydrofuran, acetonitrile, and methanol, while it was not soluble in water.

Binding Study of ZT and Hg^{2+}. To study whether ZT is able to bind with Hg^{2+}, we studied the absorption spectrum of ZT in the presence of different equivalents of Hg^{2+}. As shown in Figure 1, ZT exhibited a maximum absorption at ~361 nm

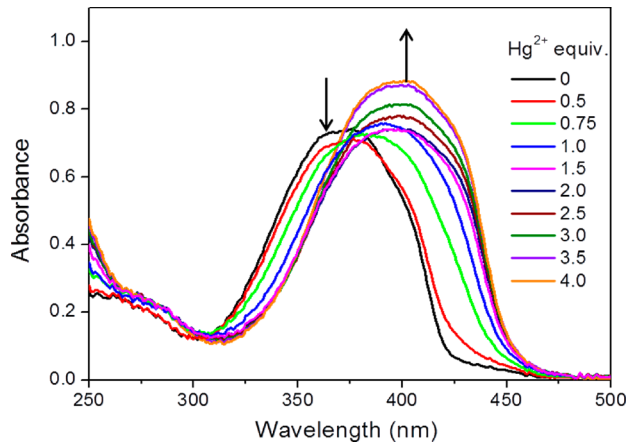

Figure 1. Absorbance response of ZT (50.0 μM) to various equivalents of Hg^{2+} in methanol.

attributed to the localized $\pi-\pi^*$ transition. Upon mixing with Hg^{2+}, the absorption at ~361 nm decreases whereas an additional absorption at ~402 nm appears. The intensity of this peak increases as the equivalents of Hg^{2+} increases such that it can be attributed to the aggregated states formed from the ZT−Hg^{2+} complex. The Job plot in Figure 2 shows a maximum achieved when the molar fraction of Hg^{2+} in aqueous solution in 0.5, suggesting the 1:1 complexation between Hg^{2+} and ZT. The binding constant of the ZT−Hg^{2+} complex calculated by using the Benesi−Hildebrand equation is 5.79 × 10 M^{-1} (Figure 3). To further study the binding mode of the ZT−Hg^{2+} complex, we compared the ^{1}H NMR spectra of ZT and the ZT−Hg^{2+} complex. It was found that when the complexes were formed, large chemical shifts in H^a, H^b, H^f, and H^g were observed. In contrast, no obvious chemical shift of H^c, H^d, and H^e were observed. This result indicates that Hg^{2+} coordinates with the two electron rich nitrogen atoms on the pyridine moiety of ZT (Figure 4). Because the Job plot reveals the binding stoichiometry between ZT and $Hg^{2+}$is 1:1, it can be

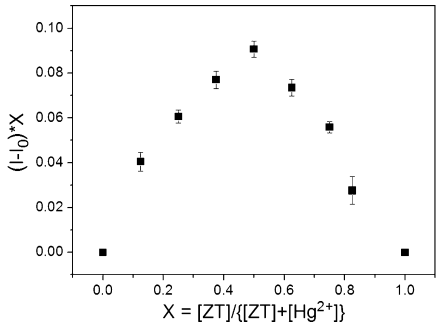

Figure 2. Job plot for ZT with Hg^{2+} in methanol. It suggests the 1:1 complexation between Hg^{2+} and ZT.

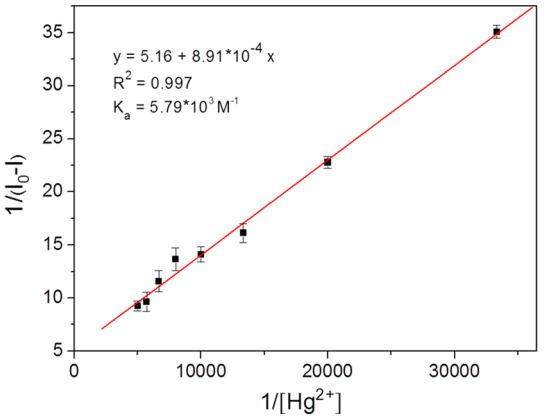

Figure 3. Benesi−Hildebrand plot of ZT with Hg^{2+} in methanol. The binding constant of the ZT−Hg^{2+} complex was calculated as 5.79 × 10^3 M^{-1}.

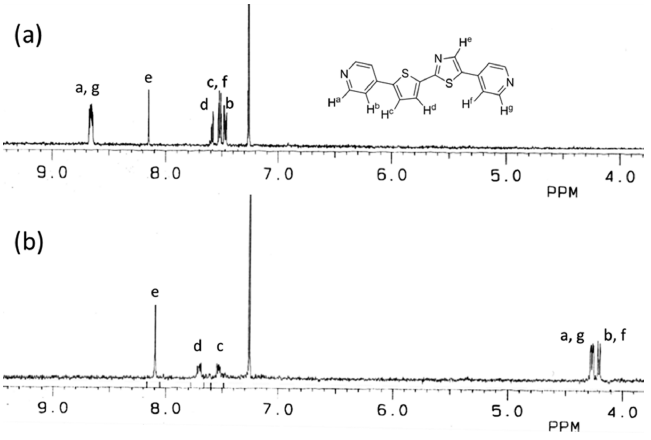

Figure 4. ^{1}H NMR spectra (300 MHz) of (a) ZT and (b) ZT−Hg^{2+} complex in $CDCl_3$. It indicates that Hg^{2+} coordinates with the two electron rich nitrogen atoms on the pyridine moiety of ZT.

suggested that two-coordinate linear ZT−Hg^{2+}complexes were formed. Such a linear binding mode was previously reported between Hg^{2+} and 4,4′-dipyridyl (Dpy), which were applied for optical detection of Hg^{2+} through the antiaggregation of gold nanoparticles.[46,47] To further study the specificity of ZT to Hg^{2+}, we performed the binding study by using another two ligands: 5-(pyridin-2-yl)-2-(5-(pyridin-2-yl)thiophen-2-yl)-thiazole (ZT-2) and 5-(pyridin-3-yl)-2-(5-(pyridin-3-yl)-thiophen-2-yl)thiazole (ZT-3). The structure of ZT-2 and ZT-3 are shown in Figure S1 in the Supporting Information.

DOI: 10.1021/acs.analchem.5b00675
Anal. Chem. 2015, 87, 4546−4551

These two ligands are structural isomers to ZT which differ from the position of nitrogen atom on the pyridine moiety. Upon the addition of Hg^{2+} to ZT-2, it was found that the maximum absorption of ZT-2 did not shift until the equivalent of Hg^{2+} is 5 times larger than ZT-2 (Figure S2 in the Supporting Information). The same phenomenon was observed upon the addition of Hg^{2+} to ZT-3 (Figure S3 in the Supporting Information). This result suggests that that only ZT is able to form a complex with Hg^{2+}. It further evidenced the linear binding mode of ZT−Hg^{2+} complexes because the metal complex was not able to form if the position of nitrogen atom on the pyridine moiety was changed.

Detection of Hg^{2+} by Using LC-Based Sensor System. After the binding of ZT with Hg^{2+} was confirmed, we applied ZT to develop an LC sensor system for detecting Hg^{2+} in aqueous solution. This system was established by placing a copper grid on a DMOAP-coated slide followed by filling the grid with 4-cyano-4′-pentyl biphenyl (5CB), a nematic LCs mostly used in current LC sensor systems, doped with 0.3% ZT as Hg^{2+} specific LCs. Then the whole system was immersed into the 0.5% SDS aqueous solution containing 5 mM Hg^{2+} or without Hg^{2+} to see whether the optical LC image will be changed in the presence of Hg^{2+}. Figure 5a shows that the optical image of LCs was bright after the system was immersed in 5 mM Hg^{2+} solution for 10 min, while Figure 5b shows that the optical image of LCs was dark in the solution without Hg^{2+} under the same conditions. Within 8 h, no obvious change for the LC images was observed. This result told us that the presence of Hg^{2+} in the solution can be detected through the dark-to-bright transition of LC images. Scheme 2 demonstrated the proposed detection mechanism of the LC/aqueous system. When there is no Hg^{2+} in the solution, the SDS molecules existing at the LC/aqueous interface align LCs homeotropically and therefore a dark LC image was observed (Scheme 2, left). The presence of Hg^{2+} leads to the formation of ZT metal complexes at the LC/aqueous interface, which disrupt the orientation of LC from homeotropic to planar and therefore a bright LC image was observed (Scheme 2, right). To further examine this phenomenon, we doped 5CB with 0.3% ZT metal complex. It was found that ZT metal complex was not able to dissolve in 5CB. Because the same amount of ZT was totally dissolved in 5CB, the reorientation of LC can be explained by the interruption of the intermolecular interaction between ZT and 5CB after ZT metal complex was formed. Besides, we also performed another two control experiments by using pure 5CB in the system. Figure 5c,d shows that both the LC images are dark no matter if Hg^{2+} was present or not, which means the presence of Hg^{2+} in the aqueous solution is not able to cause the reorientation of LCs.

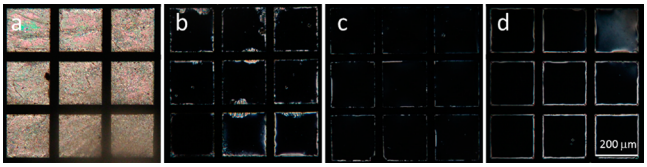

Figure 5. Polarized image of Cu grids hosting (a) 0.3% ZT doped 5CB immersed in 5 mM Hg^{2+} solution, (b) 0.3% ZT doped 5CB immersed in 0 mM Hg^{2+} solution, (c) pure 5CB immersed in 5 mM Hg^{2+} solution, and (d) pure 5CB immersed in 0 mM Hg^{2+} solution. It shows that the bright LC image appeared only when ZT and Hg^{2+} are both present in the system.

Scheme 2. Detection Mechanism of LC Sensor for Hg^{2+} Detection

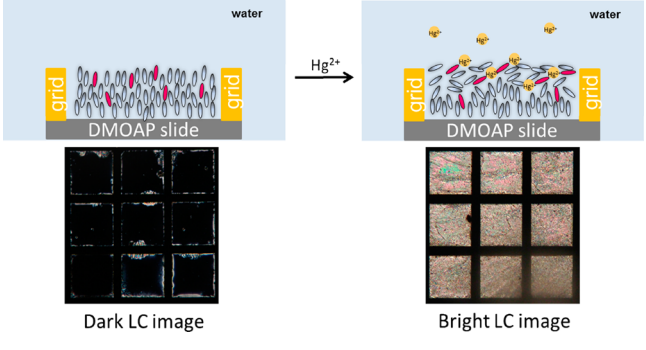

Specificity of LC-Based Sensor System for Hg^{2+} Detection. To evaluate the specificity of the LC-based sensor system, we performed the experiments by using other metal ions, including Cd^{2+}, Zn^{2+}, Cu^{2+}, Pb^{2+}, Fe^{+}, Mg^{2+}, Ca^{2+}, Na^{+}, and K^{+}, under the same experimental conditions. Cd^{2+}, Zn^{2+}, Cu^{2+}, and Pb^{2+} are also toxic metal ions while Fe^{+}, Mg^{2+}, Ca^{2+}, Na^{+}, and K^{+} are a common environmental interference which may affect the result of detection. Figure 6 shows that the optical LC image is bright only in the solution containing Hg^{2+}, while it is dark in the solution containing other metal ions. The results suggest the good specificity of this system for detecting Hg^{2+}, which can be attributed to the stronger binding affinity of ZT to Hg^{2+}. The specificity of ZT and Hg^{2+} coordination compared to main group metal ions may be attributed to the d-orbital population of Hg^{2+}.[48] This results is also consistent with previous studies showing that pyridine coordinates with Hg^{2+} more effectively than other metal ions.[47]

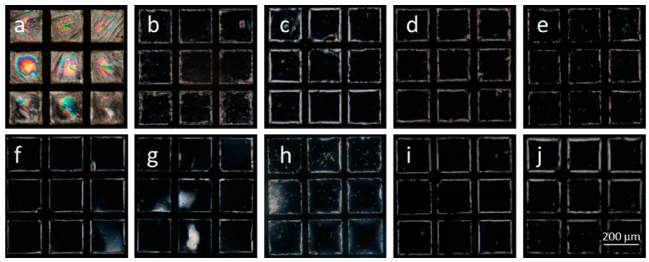

Figure 6. Polarized image of Cu grids hosting 0.3% ZT doped 5CB immersed in the aqueous solution containing 5 mM of (a) Hg^{2+}, (b) Cd^{2+}, (c) Zn^{2+}, (d) Cu^{2+}, (e) Pb^{2+}, (f) Fe^{+}, (g) Mg^{2+}, (h) Ca^{2+}, (i) Na^{+}, and (j) K^{+}. It shows that only Hg^{2+} gives a bright LC image.

Limit of Detection for Hg^{2+}. Next, we studied the limit of detection (LOD) of the system for detecting Hg^{2+} by repeating the experiments using different concentrations of Hg^{2+}. Figure 7 shows that after 10 min, the optical image of LC was bright

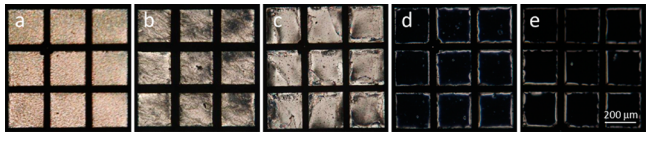

Figure 7. Polarized image of Cu grids hosting 0.3% ZT doped 5CB immersed in the aqueous solution containing (a) 500 μM, (b) 50 μM, (c) 10 μM, (d) 5 μM, and (e) 0.5 μM Hg^{2+}. It shows that the limit of detection of Hg^{2+} for this system is 10 μM.

DOI: 10.1021/acs.analchem.5b00675
Anal. Chem. 2015, 87, 4546−4551

when the concentration of Hg^{2+} is higher than 10 μM, while it remained dark when the concentration of Hg^{2+} was lower than 5 μM. On the basis of these results, we can determine the LOD for Hg^{2+} by using this system is 10 μM. This value is higher than the allowable limit in drinking water defined by the U.S. EPA (10 nM). The high LOD can be explained by the binding constant of the ZT−Hg^{2+}complex (5.79×10^3 M^{-1}) is smaller than that of other colorimetric or fluorescence-based ligands, which is mostly larger than 1×10^4 M^{-1}.[37] In addition, because the complexation of our system may only occur at the LC/aqueous interface while ZT are randomly distributed in the layer of LCs, the binding efficiency of Hg^{2+} to ZT could also be an issue for the optimized LOD of this system. However, we want to note that the feature of the LC sensor system is that there is a clear-cutoff for the bright and dark signals corresponding to a specific concentration of Hg^{2+}, which is much easier to be differentiated through the human naked-eye compared to the colorimetric or fluorescence-based sensor system of which the signals are determined by the intensity of light. This feature can be useful for regularly checking the pollution of river or pond water caused by the illegal disposal of industrial waste.

Detection of Hg^{2+} in Real Water Samples. To explore whether the developed LC sensor system can be applied for practical applications, we performed the experiments by using two real water samples: tap water and pond water. Figure 8

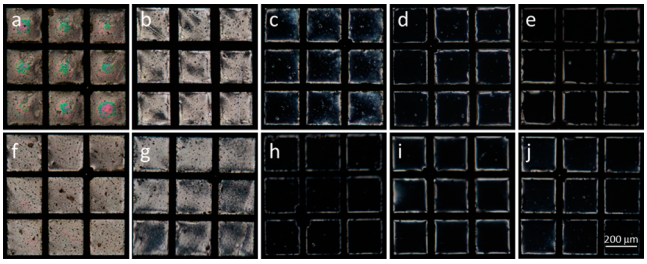

Figure 8. Polarized image of Cu grids hosting 0.3% ZT doped 5CB immersed in (a−e) tap water and (f−j) pond water containing 500, 50, 10, 5, and 0.5 μM Hg^{2+}, respectively. It shows that this system is capable of detecting 50 μM of Hg^{2+} in environmental water samples.

shows that the LOD of this system for Hg^{2+} in both tap water and pond water is 50 μM. This value is higher than the LOD of this system performed in DI water, which means the potential interference in real water samples affected the LOD of this system. This phenomenon is possibly due to the higher ionic strength of tap water and pond water than that of DI water, which stabilizes the homeotropic anchoring of LCs on the DMOAP-coated slide such that more complexes are required to disrupt the orientation of LC.[49] However, this result also demonstrated that the LC sensor system is capable of Hg^{2+} detection in environmental water samples.

CONCLUSIONS

In conclusion, we synthesized a small molecule ligand 5-(pyridin-4-yl)-2-(5-(pyridin-4-yl)thiophen-2-yl)thiazole (ZT) which forms a two-coordinate linear complex with Hg^{2+} in the ratio of 1:1. This ligand was applied to develop the LC sensor system that is simple and rapid for the portable detection of Hg^{2+} in the aqueous solution. The detection mechanism is based on the specific binding of Hg^{2+} to the ligand doped into LCs, which alters the LC reorientation and results in a dark-to-bright transition in optical signals which can be differentiated through the naked-eye. By using this system, the LOD for Hg^{2+} is 10 μM with high specificity. Besides, we also demonstrated that this system can be applied in real water samples such as tap water and pond water. The strategy using ligand-doped LCs opens the potential for the LC sensor system to detect any metal ion of interest simply by doping corresponding ligands in LCs, which makes this system suitable for fast and multiplex screening of metal ions in environmental water samples.

ASSOCIATED CONTENT

Supporting Information

Structure, synthesis, and binding studies of ZT-2 and ZT-3. This material is available free of charge via the Internet at http://pubs.acs.org.

AUTHOR INFORMATION

Corresponding Authors

*Phone: +886-2-26215656. E-mail: chc@mail.tku.edu.tw.
*E-mail: adamlee@mail.tku.edu.tw.

Notes

The authors declare no competing financial interest.

ACKNOWLEDGMENTS

We would like to thank Ministry of Science and Technology (Grant 103-2113-M-032-003-MY2) and Department of Chemistry, Tamkang University for the funding support.

REFERENCES

(1) Giller, K. E.; Witter, E.; McGrath, S. P. *Soil Biol. Biochem.* **1998**, *30*, 1389−1414.
(2) Guo, T.; Baasner, J.; Gradl, M.; Kistner, A. *Anal. Chim. Acta* **1996**, *320*, 171−176.
(3) López-García, I.; Rivas, R. E.; Hernández-Córdoba, M. *Anal. Bioanal. Chem.* **2010**, *396*, 3097−3102.
(4) Yu, L. P.; Yan, X. P. *At. Spectrosc.* **2004**, *25*, 145−153.
(5) Bagheri, H.; Gholami, A. *Talanta* **2001**, *55*, 1141−1150.
(6) Centineo, G.; González, E. B.; Sanz-Medel, A. *J. Chromatogr. A* **2004**, *1034*, 191−197.
(7) Ceulemans, M.; Adams, F. C. *J. Anal. At. Spectrom.* **1996**, *11*, 201−206.
(8) Margetínová, J.; Houserová-Pelcová, P.; Kubá, V. *Anal. Chim. Acta* **2008**, *615*, 115−123.
(9) Castillo, A.; Roig-Navarro, A. F.; Pozo, O. J. *Anal. Chim. Acta* **2006**, *577*, 18−25.
(10) Yang, F.; Li, J.; Lu, W.; Wen, Y.; Cai, X.; You, J.; Ma, J.; Ding, Y.; Chen, L. *Electrophoresis* **2014**, *35*, 474−481.
(11) Zhao, Y.; Zheng, J.; Fang, L.; Lin, Q.; Wu, Y.; Xue, Z.; Fu, F. *Talanta* **2012**, *89*, 280−285.
(12) Guo, L.; Yin, N.; Nie, D.; Fu, F.; Chen, G. *Chem. Commun.* **2011**, *47*, 10665−10667.
(13) Lou, X.; Zhao, T.; Liu, R.; Ma, J.; Xiao, Y. *Anal. Chem.* **2013**, *85*, 7574−7580.
(14) Du, J.; Sun, Y.; Jiang, L.; Cao, X.; Qi, D.; Yin, S.; Ma, J.; Boey, F. Y. C.; Chen, X. *Small* **2011**, *7*, 1407−1411.
(15) Coronado, E.; Galón-Mascarós, J. R.; Martí-Gastaldo, C.; Palomares, E.; Durrant, J. R.; Villar, R.; Grätzel, M.; Nazeeruddin, M. K. *J. Am. Chem. Soc.* **2005**, *127*, 12351−12356.
(16) So, H. S.; Rao, B. A.; Hwang, J.; Yesudas, K.; Son, Y. A. *Sens. Actuators, B* **2014**, *202*, 779−787.
(17) Nolan, E. M.; Lippard, S. J. *J. Am. Chem. Soc.* **2003**, *125*, 14270−14271.
(18) Bai, Y. Q.; Abbott, N. L. *Langmuir* **2011**, *27*, 5719−5738.

DOI: 10.1021/acs.analchem.5b00675
Anal. Chem. 2015, 87, 4546−4551

(19) Lowe, A. M.; Ozer, B. H.; Bai, Y. Q.; Bertics, P. J.; Abbott, N. L. *ACS Appl. Mater. Interface* **2010**, *2*, 722−731.
(20) Hu, Q. Z.; Jang, C. H. *Liq. Cryst.* **2014**, *41*, 597−602.
(21) Zhong, S.; Jang, C. H. *Biosens. Bioelectron.* **2014**, *59*, 293−299.
(22) Tan, L. N.; Carlton, R.; Cleaver, K.; Abbott, N. L. *Mol. Cryst. Liq. Cryst.* **2014**, *594*, 42−54.
(23) Tan, H.; Yang, S. Y.; Shen, G. L.; Yu, R. Q.; Wu, Z. Y. *Angew. Chem., Int. Ed.* **2010**, *49*, 8608−8611.
(24) Chen, C.-H.; Yang, K.-L. *Langmuir* **2010**, *26*, 1427−1430.
(25) Ding, X.; Yang, K. L. *Anal. Chem.* **2013**, *85*, 10710−10716.
(26) Chen, C.-H.; Yang, K.-L. *Anal. Biochem.* **2012**, *421*, 321−323.
(27) Liu, D.; Jang, C. H. *Sens. Actuators, B* **2014**, *193*, 770−773.
(28) Hussain, Z.; Zafiu, C.; Kupcu, S.; Pivetta, L.; Hollfelder, N.; Masutani, A.; Kilickiran, P.; Sinner, E. K. *Biosens. Bioelectron.* **2014**, *56*, 210−216.
(29) Sivakumar, S.; Wark, K. L.; Gupta, J. K.; Abbott, N. L.; Caruso, F. *Adv. Funct. Mater.* **2009**, *19*, 2260−2265.
(30) Han, G. R.; Song, Y. J.; Jang, C. H. *Colloid. Surface. B* **2014**, *116*, 147−152.
(31) Chen, C. H.; Yang, K. L. *Sens. Actuators B* **2013**, *181*, 368−374.
(32) Ding, X.; Yang, K. L. *Sens. Actuators B* **2012**, *173*, 607−613.
(33) Sutarlie, L.; Yang, K. L. *Sens. Actuators B* **2008**, *134*, 1000−1004.
(34) Hu, Q. Z.; Jang, C. H. *Colloids Surf., B* **2011**, *88*, 622−626.
(35) Yang, S.; Wu, C.; Tan, H.; Wu, Y.; Liao, S.; Wu, Z.; Shen, G.; Yu, R. *Anal. Chem.* **2013**, *85*, 14−18.
(36) Nolan, E. M.; Lippard, S. J. *Acc. Chem. Res.* **2009**, *42*, 193−203.
(37) Nolan, E. M.; Lippard, S. J. *Chem. Rev.* **2008**, *108*, 3443−3480.
(38) Han, A.; Liu, X.; Prestwich, G. D.; Zang, L. *Sens. Actuators, B* **2014**, *198*, 274−277.
(39) Yu, S. Y.; Wu, S. P. *Sens. Actuators, B* **2014**, *201*, 25−30.
(40) Neupane, L. N.; Thirupathi, P.; Jang, S.; Jang, M. J.; Kim, J. H.; Lee, K. H. *Talanta* **2014**, *85*, 1566−1574.
(41) Nolan, E. M.; Lippard, S. J. *J. Am. Chem. Soc.* **2007**, *129*, 5910−5918.
(42) Wu, X. F.; Ma, Q. J.; Wei, X. J.; Hou, Y. M.; Zhu, X. *Sens. Actuators, B* **2013**, *183*, 565−573.
(43) Clem, T. A.; Kavulak, D. F. J.; Westling, E. J.; Fréchet, J. M. J. *Chem. Mater.* **2010**, *22*, 1977−1987.
(44) Lee, A. S. Y.; Dai, W. C. *Tetrahedron* **1997**, *53*, 859−868.
(45) Benesi, H. A.; Hildebrand, J. H. *J. Am. Chem. Soc.* **1949**, *71*, 2703−2707.
(46) Li, Y.; Wu, P.; Xu, H.; Zhang, Z.; Zhong, X. *Talanta* **2011**, *84*, 508−512.
(47) Du, Y.; Liu, R.; Liu, B.; Wang, S.; Han, M. Y.; Zhang, Z. *Anal. Chem.* **2013**, *85*, 3160−3165.
(48) Rodgers, M. T.; Stanley, J. R.; Amunugama, R. *J. Am. Chem. Soc.* **2000**, *122*, 10969−10978.
(49) Carlton, R. J.; Gupta, J. K.; Swift, C. L.; Abbott, N. L. *Langmuir* **2012**, *28*, 31−36.

DOI: 10.1021/acs.analchem.5b00675
Anal. Chem. 2015, 87, 4546−4551